An EMI Estimate for Shielding Enclosure Design

M. Li, S. Radu*,
J. L. Drewniak, T. H. Hubing, T. P. VanDoren, and R. E. DuBruff
University of Missouri–Rolla, USA; *Sun Microsystems, Inc., USA

Abstract: A relatively simple, closed-form expression was developed to estimate the EMI from perforated shielding enclosures based on coupling from interior sources through slots and apertures at enclosure cavity modes [1]. A power balance method [2], Bethe's small hole theory [3], and empirically developed formulae for the relation between radiation and slot length and number of slots, were employed to estimate an upper bound on the radiated EMI from shielding enclosures. Comparisons between measurements and estimated field strengths suitably agree within engineering accuracy.

1. Introduction

It is difficult to meet EMC requirements for high-speed digital electronic products without a shielding enclosure. The integrity of shielding enclosures is compromised by slots and apertures for heat dissipation, CD-ROMs, I/O cable penetration, and plate-covered unused connector holes, among other things. Radiation from slots and apertures in conducting enclosures, excited by interior sources, is of great concern in meeting radiated EMI requirements. From previous studies, it was found that cavity mode resonances can result in significant radiation through electromagnetically short slots [1]. Estimating the EMI from a shielding enclosure through slots or apertures is a critical aspect in anticipating EMI problems in a product design.

Radiation from conducting cavities at frequencies below cavity-mode resonances has been investigated experimentally and numerically [4], [5], [6], [7]. Recent work determined the tangential electric fields from simulations and measurements, then applied equivalence principles to estimate the radiation from apertures [8]. The effect of aperture area on shielding effectiveness has also been studied [9]. A power balance method to estimate Qs of resonances associated with shielded enclosures has also been reported [2]. Much of the work done to date employs simulations that require significant computational resources and time, and may only be suitable for simple or ideal cases. A relatively simple closed-form expression for estimating the radiated EMI from shielding enclosures based on both analytical and empirical developments is reported herein.

An ideal rectangular cavity was first analyzed, using a power balance method. The interior electronics were treated as a factor affecting the Q of the shielding enclosure. Then the slots were modeled as radiation sources using Bethe's small hole theory for slots less than $\frac{1}{3}\lambda$. The mode numbers were ignored for simplicity. Though the EMI estimate is based on a simple model, the comparison between the measurements and calculations is acceptable for engineering development.

2. An EMI Estimate

A shielding enclosure has resonances associated with its dimensions. In practice, the exterior of shielding enclosures are often rectangular. However, the interior is broken up by PCB conducting planes, plug-in modules, large heatsinks, sub-enclosures for power supplies, or any number of other aspects of an electronic product. These aspects will affect resonance frequencies and cavity Qs. From an engineering perspective, however, predicting a specific resonance frequency is not necessary. With so much complexity in the enclosure interior, these frequencies will shift in the course of the many changes that are a natural part of any design cycle. An estimate of the envelope or upper bound of the radiation due to interior sources is desirable in engineering design in order to guide decisions on the size and number of slots and apertures. The approach detailed below proceeds from simple cavity theory, making assumptions along the way regarding the modes, source, and cavity Q, which are guided by measurements.

The Bethe small-hole theory interprets the aperture as a radiating magnetic dipole $\vec{M}$ along the hole plane, and an electric dipole $\vec{P}$ along the normal direction to the hole plane [3]. The $\vec{M}$ and $\vec{P}$ are related to the short-circuited magnetic field in the hole plane $\vec{H_0}$, and the normal short-circuited electric field $\vec{E_0}$ as

$$\vec{M} = P_m \vec{H_0} \tag{1}$$

$$\vec{P} = P_e \vec{E_0} \tag{2}$$

where P_m and P_e are the magnetic and electric polarizabilities, respectively. The electric dipole has no contribution to the electric far field at the observation points in front of the aperture panels, which is

$$|E_{far}| = \eta \frac{\omega^2}{2\pi c^2 R} \vec{M} \tag{3}$$

where η is the wave impedance, $\omega = 2\pi f$ (f is the frequency), c is the speed of light, and R is the distance between the source and observation point.

The magnetic polarizability for a slot with length L and width W can be found in the literature on microwave coupling as [12]

$$P_m = \frac{0.132}{ln(1 + \frac{0.66}{\alpha})} L^3, \tag{4}$$

where α is the ratio of slot length L to slot width W. The magnetic polarizability for a circular aperture is [13]

$$P_m = \frac{4}{3} a^3, \tag{5}$$

where a is the radius of the circular aperture. According to Equations (4) and (5), the magnetic polarizability of a square aperture is equivalent to that of a circular aperture with the same area within 0.7 dB. Bethe's expression can then be augmented for small apertures with length L and width W as

$$|E_{far}| = 7.9 \frac{\omega^2 L^3 |H|}{c^2 R \; ln(1 + 0.66\alpha)}. \tag{6}$$

For an ideal rectangular enclosure of width a, height b, and depth d, an arbitrary interior field due to sources can be expanded in TM and TE modes. The distribution of interior fields and currents on the interior walls can also be calculated for each cavity mode [2][10]. The interior fields for a $TM_z(mnp)$ mode for an ideal rectangular cavity are given analytically [10]. The total energy W stored in a particular mode is related to the fields through the magnetic energy W_μ as

$$W = 2W_\mu = 2A_{mnp}^2 \frac{\mu_0}{4} \int |\vec{H}|^2 dv$$

$$= A_{mnp}^2 \frac{\mu_0}{2} \int_0^a \int_0^b \int_0^d (H_x^2 + H_y^2) dx dy dz$$

$$= A_{mnp}^2 n_g \frac{V}{8\mu_0} (\beta_x^2 + \beta_y^2) \tag{7}$$

where $\beta_x = \frac{m\pi}{a}$, $\beta_y = \frac{n\pi}{b}$, $n_g = 1$ for $p = 0$, and $n_g = 1/2$ for $p \neq 0$, $V = abd$ is the volume of the enclosure, and A_{mnp} is the modal coefficient.

The Q of an enclosure is defined as the ratio of time-averaged energy stored in the cavity, to the energy dissipated in the enclosure in one period. The stored energy is related to the Q through

$$W = \frac{P_0 Q}{\omega} = A_{mnp}^2 n_g \frac{V}{8\mu_0} (\beta_x^2 + \beta_y^2), \tag{8}$$

where P_0 is the power delivered to the enclosure. The constant A_{mnp} can then be determined. For a slot along the x direction in the face $z = 0$ or $z = d$, the field contributing to the radiation measured in front of the face containing the slot is H_x, and

$$H_x = \frac{A_{mnp} \beta_y}{\mu_0} = [\frac{8 P_0 Q}{n_g \mu_0 \omega V (\frac{\beta_x^2}{\beta_y^2} + 1)}]^{1/2}. \tag{9}$$

The far-field radiation at distance R using Eq.(6) in Bethe's small hole theory is then

$$|\vec{E}|_{far} = \frac{22.3 \omega^{3/2} L^3}{c^2 R ln(1 + 0.66\alpha)} [\frac{P_0 Q}{n_g \mu_0 V (\frac{\beta_x^2}{\beta_y^2} + 1)}]^{1/2}. \tag{10}$$

Empirically including the number of slots N (justified in a later section), the approximate far electric field is

$$|E_{far}| = N \frac{22.3 (2\pi)^{3/2} L^3 f^{3/2}}{ln(1 + 0.66\alpha) c^2 R} [\frac{P_0 Q}{n_g \mu_0 V (\frac{\beta_x^2}{\beta_y^2} + 1)}]^{1/2}. \tag{11}$$

Assuming all the available power is delivered to the enclosure, i.e.,

$$P_0 = \frac{V_s^2}{8 R_s}, \tag{12}$$

where V_s is the noise voltage, and R_s is the noise source impedance, and assuming the mode numbers β_x and β_y are close to each other, an EMI estimate is

$$|E_{far}| = \frac{7.9 (2\pi)^{3/2} N V_s L^3 f^{3/2}}{ln(1 + 0.66\alpha) \sqrt{\mu_0} c^2 R} \sqrt{\frac{Q}{R_s V}}. \tag{13}$$

At $R = 3$ m, expressing all terms in mks units, the estimate can be expressed in the following simplified form,

$$|E_{far}| = 4.1 \times 10^{-13} \frac{N V_s L^3 f^{3/2}}{ln(1 + 0.66\alpha)} \sqrt{\frac{Q}{R_s V}}. \tag{14}$$

At $R = 3$ m, Eq.(14) then gives an estimate for the envelope of radiated EMI from an enclosure that includes the frequency dependence, number of slots or apertures, perforation dimensions, enclosure volume and Q, and the source properties. The location of the source is not specified because an approximate worst-case envelope independent of source position is sought. Hence, all of the available power from the source is used. At resonances, this is a reasonable worst-case approximation.

The dependence on the number and dimensions of the slots (or apertures) is demonstrated with measurements in the next section. A range for the enclosure Q was also determined using a production populated PCB in an enclosure. In general, estimating the noise source voltage V_s, and real part of the source impedance R_s, is among the most difficult aspects of applying the developed EMI estimate. An EMI estimate identical to that in Eq.(13) can also be developed for TE modes.

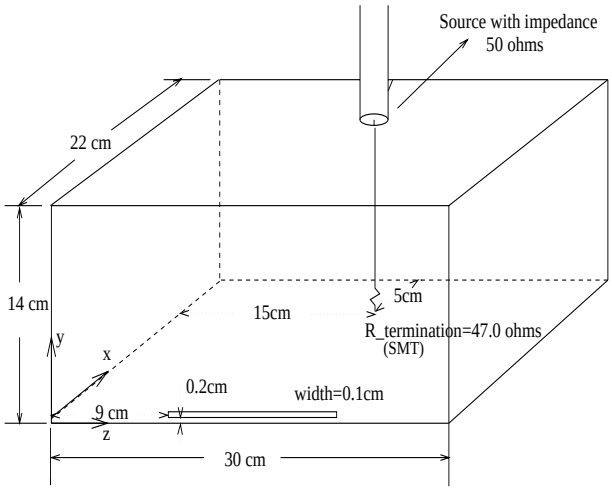

Figure 1: Geometry of the small test enclosure

3. Corroborating and Applying the EMI Estimate

The factors for N (the number of slots), Q, L (the slot length), and the absence of terms for the source size, polarization and location require further justification in applying the EMI estimate in Eq.(13). Measurements and finite-difference time-domain (FDTD) modeling were both used for this purpose. The EMI estimate was then applied to a testbed designed to approximate a SUN S-1000E server that included the motherboard and plug-in modules. Swept frequency measurements with a known source to approximate a power coupling path in the functional electronics demonstrates the utility of the approach.

Two test enclosures were studied. One was a 20-cm $\times$ 14-cm $\times$ 30-cm cavity excited by a feed probe terminated with a 47-Ω resistor, shown in Figure 1. The resistor was introduced to provide the necessary loss for FDTD modeling. The other enclosure was a 40-cm $\times$ 20-cm $\times$ 50-cm enclosure that mimicked the dimensions of a Sun S-1000E server. A patch source driven against the top of the enclosure was used to approximate a noise source driving a heatsink in the real product, which was determined to be the primary coupling path for CPU harmonics [11] . Two-port S-parameters were measured in a semianechoic chamber, where the source in the enclosure under test was connected to Port 1 of a Wiltron 37247A network analyzer, and a horn antenna outside the enclosure was connected to Port 2. Measurements were made at 3 m, which is effectively the far-field at the frequencies of the enclosure resonances. The network analyzer was placed outside the semianechoic chamber and configured to measure the reflection coefficient $|S_{11}|$, and the transmission coefficient $|S_{21}|$. The electric field is calculated from $|S_{21}|$ and the antenna factor AF of the antenna at 3 m as

$$|\vec{E}|_{far} = V_{in} \times |S_{21}| \times AF = \frac{1}{2} V_s \times |S_{21}| \times AF. \quad (15)$$

In the functioning S-1000E, the sides were small-hole airflow aperture arrays that did not contribute appreciably to the radiated EMI, and the top and bottom had no perforations. Several front- and back-panel configurations of the S-1000E type test enclosure were constructed to study various aspects of the EMI estimate Eq.(13). Radiated EMI measurements were then made broadside to the front and back faces.

The Q of the enclosure is an important factor in Eq.(13). An approximate range of the Q for enclosures with interior electronics is needed in order to apply Eq.(13). Measurements of the S-1000E test enclosure were made with and without unpopulated and populated motherboards. An array of fifteen 4-cm slots were located on the enclosure front and back faces as the radiators. The Q at enclosure resonances for the empty test enclosure was as high as 1000. The loading effect of the unpopulated S-1000E motherboard was minimal, however, the loading of the populated motherboard was significant. The Q was calculated as the ratio of the resonance frequency to the half-power bandwidth of that resonance. From the measurements, the Q for the test enclosure loaded with a populated motherboard ranged from 10 to 50 at resonances up to approximately 2 GHz.

The dependence of the interior source size, polarization, and location was also studied experimentally. An arbitrary interior field can be expanded in terms of a complete set of enclosure modes, if the modes are known [13]. The modal coefficients of the expansion are given as the inner product of the particular mode and the Maxwellian sources. Consequently, the location, size, and polarization of the effective interior source driving the enclosure, or the "EMI antenna" will have a significant impact on the amplitude of any given resonance frequency. Further, the location of the EMI antenna, e.g., a heatsink, is a boundary condition that affects the modal resonance frequencies. However, an EMI envelope is desired here for use in design. Several source geometries including a protruding monopole, PCB traces, and various size patches driven against the enclosure and PCB were studied experimentally at numerous locations over three orthogonal enclosure walls. The amplitude of any given resonance was a strong function of the source shape, size, and location. However, once the source protruded $1-2$ cm above a PCB, and had dimensions greater than $\frac{1}{10}\lambda$, it became an effective source for driving the enclosure. At that point the envelope of the radiation peaks did not shift up or down appreciably, though individual peaks did.

Consequently, the source location, size, and polarization are not included in the EMI estimate. Each of these parameters has no effect on the envelope of the radiated emissions. This is fortuitous for practical applications, since the enclosure design is developed concurrently or prior to the interior electronics.

A single slot with varying slot length on the small test enclosure was investigated to demonstrate the L^3 relation of EMI and slot length. Measurements as well as FDTD modeling were both applied, and the

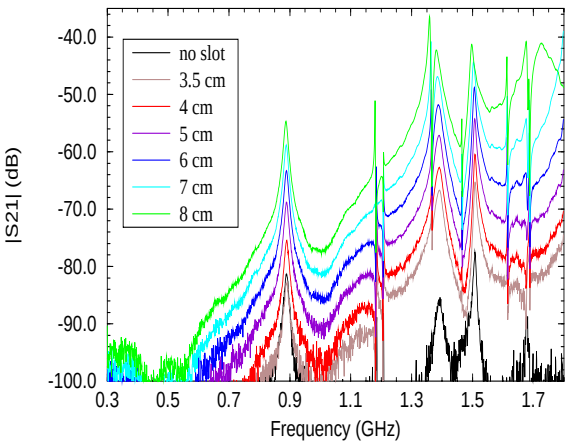

Figure 2: The radiation from a single slot with varying slot length.

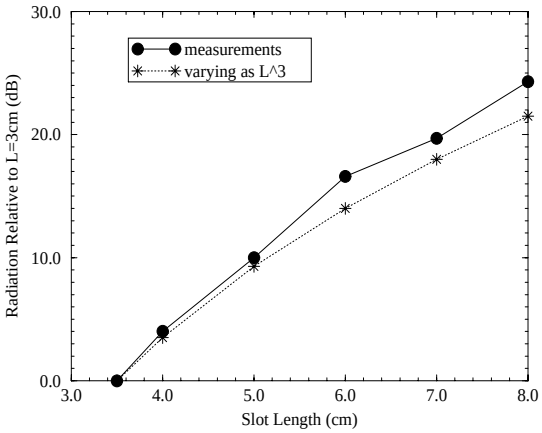

Figure 3: The relation of EMI to slot length for a single slot.

agreement was good, with a maximum difference of 2 dB for the far fields up to 2.2 GHz. The FDTD results are omitted in the following for clarity. The delivered power for slot lengths of 3.5 cm, 4 cm, 5 cm, 6 cm, 7 cm, and 8 cm was measured up to 1.8 GHz, and was not affected by the slot, except the 8 cm slot which is $\frac{1}{3}\lambda$ long at 1.2 GHz. The cavity modes are the coupling paths. The presence of the slot did not appreciably change the cavity mode resonances, i.e., the radiated power is only a fraction of the power dissipated in the enclosure.

The $|S_{21}|$ measurements are shown in Figure 2. It is clear that the radiation spectrum does not change with slot length (except the 8 cm slot). Again, demonstrating that the power radiated from the slot, which is coupled through the cavity modes, is only a small part of the power delivered to the enclosure. The EMI increase at the first few resonances TM_y101, TM_y111, and TM_y201 as a function of slot

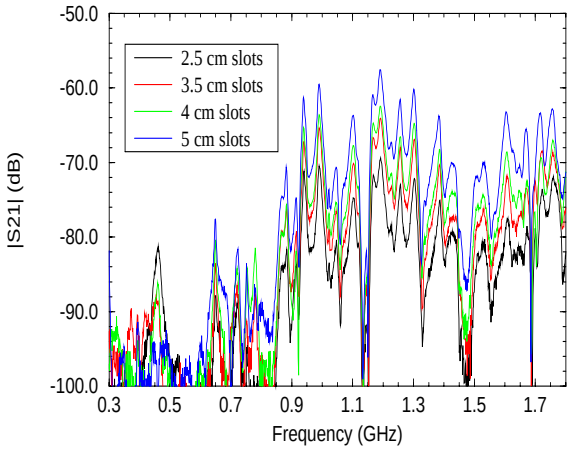

Figure 4: Radiation from the S-1000E test enclosure excited by a patch source and loaded with the populated S-1000E motherboard.

length is summarized in Figure 3. The curve for L^3 is also given normalized to the radiation from the slot with length 3.5 cm. The agreement is good, with the largest deviation being 2 dB for the 8 cm slot.

The slots on the front and rear panels of the S-1000E test enclosure were designed to mimic the seams in the S-1000E shielding enclosure. A set of slots with lengths of 5 cm, 4 cm, 3.5 cm, and 2.5 cm were successively measured. The enclosure was excited by a patch source, and the populated S-1000E motherboard was placed in the interior. The results for the receiving antenna facing the front panel are shown in Figure 4. The increments in radiation from short slots to long slots were generally uniform at all frequencies, with an average value of 5 dB for 2.5-cm slots increased to 3.5-cm slots, 2-dB for 3.5-cm slots to 4-cm slots, and 4 dB for 4 cm slots to 5-cm slots. The increments varying as NL^3 would be 5.8 dB, 1.6 dB, and 4.2 dB. Again, the agreement is generally good.

The EMI is directly proportional to the number of slots N in Eq.(13). Measurements and FDTD modeling on two 6-cm slots end-to-end, and two or three 6-cm slots side-by-side in the small test enclosure showed that the radiation from two slots was 6 dB (2 times) greater than the radiation from a single slot. The radiation from three short slots in parallel was approximately 10 dB (3 times) greater than the radiation from a single slot. Measurements on the S-1000E test enclosure for increasing numbers of apertures in an aperture array (28 to 252 apertures) on one face also showed that the radiation was directly proportional to the number of apertures, as shown in Figure 5. The aperture size for the results in Figure 5 was 1 $cm \times 1$ cm. However, arrays of 1.5 cm, 2 cm, 2.5 cm, and 3 cm size apertures were also studied experimentally and numerically with the same conclusion. For real situations with complicated slot length and aperture distributions, the factor NL^3

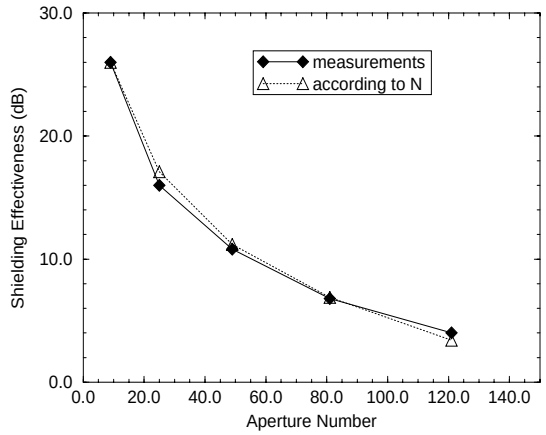

Figure 5: Relative shielding effectiveness from multiple apertures for 1 cm square apertures.

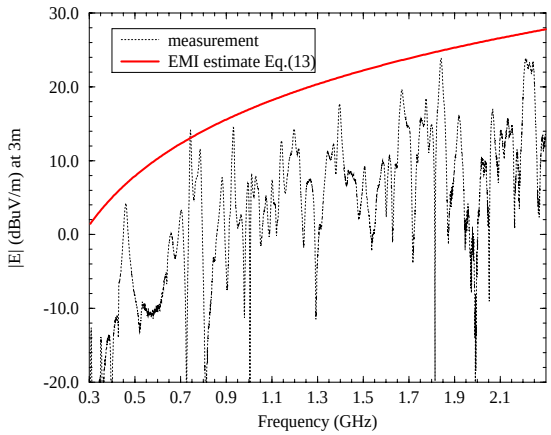

Figure 6: Comparison of measurements and the EMI estimate for the S-1000E test enclosure excited by a patch source, with a populated motherboard in the interior.

for the differing size would be treated independently and summed. The polarization of the slots should also be considered, i.e., for horizontal electric fields, N in Eq.(13) is the number of vertical slots, and vice versa for vertical electrical fields.

Eq.(13) was applied to estimate the electric field at 3 m from the S-1000E test enclosure excited with a patch source and loaded with the populated S-1000E motherboard. A comparison between measurements and the estimated field is shown in Figure 6. The source in this case is well-known with $V_s = 1\ mV$, and $R_s = 50\ \Omega$ for the network analyzer. The Q used in the EMI estimate curve was 15. All factors in Eq.(13) were then determined prior to plotting the EMI estimate (i.e., it is not a fitted curve). The simple heuristically developed closed-form expression sufficiently estimates the envelope of the the radiated field strength at enclosure resonances. Numerically modeling the complicated enclosure geometry including the populated motherboard in this situation is not practical. However, the EMI estimate in Eq.(13) provides useful guidance for enclosure design.

4. Summary and Conclusions

EMI from electrically short slots and small apertures results from the coupling of interior sources through enclosure cavity modes. Radiation from shielding enclosures through slots and apertures was estimated from a simple heuristically determined closed-form expression, using Bethe's small-hole coupling theory. The estimate explicitly contains the functional variation of EMI with frequency, number and dimensions of perforations (slots and contains the functional variation of EMI with frequency, number and dimensions of perforations (slots and apertures), enclosure volume, cavity Q, and the noise source voltage and real part of the impedance. Measurements and FDTD modeling were applied to develop and corroborate aspects of the estimate. Agreement between measurements for known V_s and R_s and the estimate was sufficient for application in engineering design.

The estimate has been developed based on electrically short slots, though it works for $L < \frac{\lambda}{3}$. The demonstrated EMI variation with L can be used in design for reducing slot length to achieve a desired reduction in radiated EMI. This minimizes over-design and reduces the costly application of finger-stock or EMI gasketing. The factor L^3N is also being used by the authors for an air-flow aperture array design.

Although this estimate is a useful tool for designing and evaluating shielding enclosures, a shortcoming of this approach is the current lack of knowledge regarding the source properties V_s and R_s for the estimate. Active IC sources at the PCB level will typically couple to large structures such as a heatsink or other conductors of significant electrical extent. The authors are currently developing models that can be used to estimate V_s and R_s for this type of source.

References

[1] M. Li, S. Radu, Y. Ji, J. Nuebel, W. Cui, J. L. Drewniak, T. H. Hubing, T. P. VanDoren, "EMI from apertures at enclosure cavity mode resonances", *IEEE Trans. Electromagn. Compat. Symp.*, pp.183-187, 1997.

[2] D. A. Hill, M. T. Ma, A. R. Ondrejka, B. F. Riddle, M. L. Crawford, R. T. Johnk, "Aperture excitation of electrically large, lossy cavities", *IEEE Trans. Electromagn. Compat.*, vol. 36, pp.169-177, August 1994.

[3] H. A. Bethe, "Theory of diffraction by small holes", *Physical Review*, vol. 66, pp. 163-182, 1944.

[4] S. Daijavad and B. J. Rubin, "Modeling common-mode radiation of 3D structures", *IEEE Trans. Electromagn. Compat.*, vol. 34, pp. 57-61, February 1992.

[5] S. Hashemi-Yeganeh and C. Birtcher, "Theoretical and experimental studies of cavity-backed slot antenna excited by a narrow strip", *IEEE Trans. Antennas Propagat.*, vol. 41, pp. 236-241, February 1993.

[6] J. Y. Lee, T. S. Horng and N. G. Alexopoulos, "Analysis of cavity-backed aperture antennas with a dielectric overlay", *IEEE Trans. Antennas Propagat.*, vol. 42, pp. 1556-1561, November 1994.

[7] H. A. Mendez, "Shielding theory of enclosures with apertures," *IEEE Trans. Electromagn. Compat.*, vol. 20, pp.296-305, May 1978.

[8] G. Cerri, R. D. Leo, and V. M. Primiani, "Theoretical and experimental evaluation of the electromagnetic radiation from apertures in shielded enclosure," *IEEE Trans. Electromagn. Compat.*, vol. 34, pp.423-432 November 1992.

[9] H. Y. Chen, I-Y. Tarn, and Y-J. He, "NEMP fields in side a metallic enclosure with an aperture in one wall,", *IEEE Trans. Electromagn. Compat.*, vol. 37, pp.99-105, February 1995.

[10] C. A. Balanis, *Advanced Engineering Electromagnetics;* John Wiley & Sons; New York, 1989.

[11] S. Radu, Y. Ji, J. Nuebel, J. L. Drewniak, T. P. Van Doren, and T. H. Hubing, "Identifying an EMI source and coupling path in a computer system with sub-module testing", *IEEE Electromagnetic Compatibility Symposium Proceedings,* pp. 165-170, Austin, TX, 1997.

[12] N. A. McDonald, "Simple approximations for the longitudianl magnetic polarizabilities of some small apertures", *IEEE Trans. Microw. The. Tech.*, vol. 36, pp. 689-695, July 1988.

[13] R. E. Collin, *Field Theory of Guided Waves*; IEEE press; 1991.